Resonance-modulated wavelength scaling of high-order-harmonic generation from H_2^+

Baoning Wang,[1] Lixin He,[1,*] Feng Wang,[1] Hua Yuan,[1] Xiaosong Zhu,[1] Pengfei Lan,[1,†] and Peixiang Lu[1,2,‡]

[1]*School of Physics and Wuhan National Laboratory for Optoelectronics, Huazhong University of Science and Technology, Wuhan 430074, China*

[2]*Laboratory of Optical Information Technology, Wuhan Institute of Technology, Wuhan 430205, China*

(Received 6 December 2017; published 22 January 2018)

Wavelength scaling of high-order harmonic generation (HHG) in a non-Born-Oppenheimer treatment of H_2^+ is investigated by numerical simulations of the time-dependent Schrödinger equation. The results show that the decrease in the wavelength-dependent HHG yield is reduced compared to that in the fixed-nucleus approximation. This slower wavelength scaling is related to the charge-resonance-enhanced ionization effect, which considerably increases the ionization rate at longer driving laser wavelengths due to the relatively larger nuclear separation. In addition, we find an oscillation structure in the wavelength scaling of HHG from H_2^+. Upon decreasing the laser intensity or increasing the nuclear mass, the oscillation structure will shift towards a longer wavelength of the laser pulse. These results permit the generation of an efficient harmonic spectrum in the midinfrared regime by manipulating the nuclear dynamics of molecules.

DOI: 10.1103/PhysRevA.97.013417

I. INTRODUCTION

High-order-harmonic generation (HHG) is considered to be essential to generating extreme ultraviolet to soft x-ray radiation [1,2] and attosecond pulses [3–7], which provide an important tool for tomographic imaging molecular structure [8–11] and probing electronic dynamics in atoms, molecules, and solids with unprecedented resolution [12–14]. The mechanism of HHG can be understood by a semiclassical three-step model: removal of an electron by an intense laser pulse, acceleration of the electron in the laser field, and recombination with the parent ion [15,16]. The maximum harmonic energy is given by the cutoff law $E_{\max} = I_p + 3.17U_p$ [15,16], where I_p donates the ionization potential of the target atom or molecule, and $U_p \propto I\lambda^2$ is the ponderomotive energy, with I the laser electric field intensity and λ the wavelength of the laser pulse.

In the past decades, considerable effort has been devoted to extending the cutoff energy so that the much shorter attosecond pulse can be generated. According to the cutoff law, the intensity is an obvious experimental control parameter to extend the cutoff, but it is limited by the saturation of ionization. In this context, using a longer wavelength has the advantage that more energetic photons can be generated. Recently developed optical parametric amplification techniques [17–19] triggered a growing interest in the investigation of the HHG process in midinfrared laser pulses [20,21]. For example, using a 1.6-μm driving laser pulse, Takahashi *et al.* have reported the generation of harmonics in the "water window" region [21]. However, recent theoretical calculations and experimental observations have revealed a much faster decrease in the HHG yield from atoms, which scales as $\lambda^{(5-6)}$ [22–27]. This will be a major hurdle for generating intense HHG in the water window with midinfrared laser pulses. In order to slow down this trend, several schemes have been proposed, e.g., using optically prepared excited-state atoms [28] or a two-color field [29].

Compared to HHG in atoms, molecular high-order-harmonic generation demonstrates more complicated and more interesting features due to the rich internal structure of the molecule and additional freedom of the nuclear motion, such as the structure or dynamic minimum [30–34], the shape resonance [35], and the amplitude [36–38] and frequency [39,40] modulations in the spectrum. Recently, the wavelength scaling of a molecular high harmonic yield has attracted a lot of attention [41–43]. Li *et al*. study the influence of the molecular structure and electron dynamics on the wavelength scaling of HHG from aligned molecules [41]. Yue *et al*. investigate the wavelength dependence of HHG yield in H_2^+ with the fixed-nucleus approximation [42]. Liu *et al*. find that ground-state depletion could result in a dramatic decrease in the wavelength scaling of HHG from H_2^+ [43]. Moreover, Zuo and Bandrauk demonstrate that nuclear motion will induce charge-resonance-enhanced ionization (CREI), which will significantly modulate the HHG yield [44–50]. However, this effect has scarcely been investigated in previous studies of wavelength scaling in molecular high-order-harmonic generation.

In this paper, we theoretically investigate the CREI effect on the wavelength scaling of HHG from H_2^+ by numerically solving the non-Born-Oppenheimer (non-BO) time-dependent Schrödinger equation (TDSE). We find that the molecular harmonic yield decreases more slowly than that in the fixed-nucleus approximation. This is because H_2^+ driven by laser pulses with longer wavelengths can move to larger internuclear distances, where the CREI effect can significantly improve the ionization rate and therefore the HHG yield. Besides, an oscillation structure in the wavelength scaling is observed. By decreasing the intensity of the laser pulse or increasing the mass

*helx@mail.hust.edu.cn
†pengfeilan@mail.hust.edu.cn
‡lupeixiang@mail.hust.edu.cn

of nuclei, we have demonstrated that the oscillation structure in the wavelength scaling moves towards a longer wavelength of the driving laser pulse.

II. THEORETICAL MODEL

We investigate HHG in a non-BO treatment of H_2^+ by numerically solving the TDSE [51,52]. In our simulation, the H_2^+ molecular ion is assumed to be aligned along the polarization direction of the linearly polarized laser pulses. Rotational motion of the molecules and transversal spreading of electronic wave function are not included. The TDSE is expressed as (Hartree atomic units are used throughout)

$$i\frac{\partial}{\partial t}\psi(R,z;t) = [H_0 + V(t)]\psi(R,z;t), \tag{1}$$

where H_0 is the field-free Hamiltonian:

$$\begin{aligned} H_0 &= T + V_0 \\ &= -\frac{1}{2\mu}\frac{\partial^2}{\partial R^2} - \frac{1}{2\mu_e}\frac{\partial^2}{\partial z^2} - \frac{1}{\sqrt{(z-R/2)^2+\alpha}} \\ &\quad - \frac{1}{\sqrt{(z+R/2)^2+\alpha}} + \frac{1}{\sqrt{R^2+\beta}}. \end{aligned} \tag{2}$$

Here, R is the internuclear distance, z is the electron position measured from the center of mass of two protons, and $\mu = m_p/2$ and $\mu_e = 2m_p/(2m_p+1)$ are the reduced masses (m_p is the mass of the proton). $\alpha = 1$ and $\beta = 0.03$ are the soft-core parameters. In the dipole approximation, the length-gauged laser-molecule interaction is $V(t) = [1 + 1/(2m_p+1)]zE(t)$. We solve Eq. (1) by using the Crank-Nicolson method [51,52]. To eliminate artificial reflections from boundaries, the wave function is multiplied by a $\sin^{1/6}$-masking function at each time step. The initial state is the ground state $1s\sigma_g$ of H_2^+, which is obtained by using the imaginary time propagation method of the field-free TDSE. The equilibrium internuclear distance is given by $R_e = \frac{\langle\psi_0|R|\psi_0\rangle}{\langle\psi_0|\psi_0\rangle}$ (ψ_0 is the initial wave function). The harmonic spectrum is obtained by the Fourier transformation of the dipole acceleration $a(t) = \langle\psi(t)|-\frac{\partial V_0}{\partial z} + E(t)|\psi(t)\rangle$. For comparison, we also solve Eq. (1) with the internuclear distance fixed at R_e, which is called the static case in the following.

III. RESULTS AND DISCUSSION

In our simulations, the driving pulse is chosen to be a five-cycle flat-top laser pulse with one-cycle linear ramps of turn on and turn off. The wavelength scaling of the HHG yield is calculated with the laser wavelength changing from 750 to 2000 nm. The harmonic yield $\Delta I(\lambda)$ is obtained by integrating the harmonic spectrum intensity $S(\omega)$ from $I_p + U_p$ to $I_p + 2U_p$:

$$\Delta I(\lambda) \propto \frac{1}{U_p}\int_{I_p+U_p}^{I_p+2U_p} S(\omega)d\omega. \tag{3}$$

In the non-BO treatment (moving H_2^+), the increasing internuclear separation of H_2^+ can lead to a decrease in the ionization potential I_p [49]. Therefore, the harmonic cutoff energy in the moving H_2^+ is lower than that in the static case,

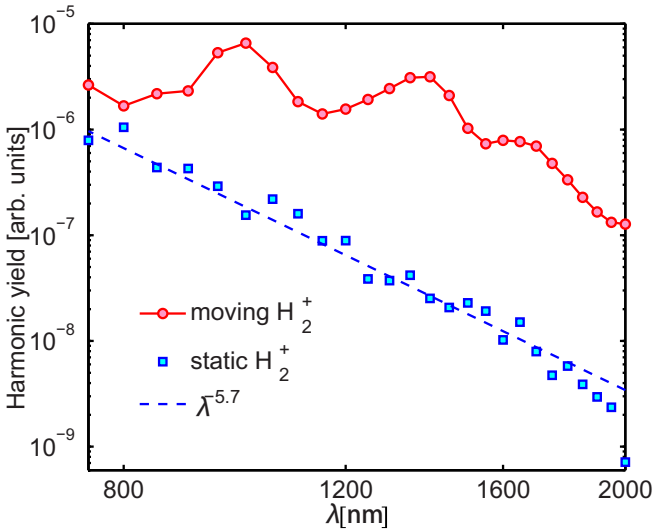

FIG. 1. . Wavelength scaling of H_2^+ by solving the TDSE in non-BO treatment (red circles with line) and in the fixed-nucleus approximation (blue squares).

i.e., $I_p + 3.17U_p$ [see Fig. 2(b)]. In our simulations, the upper limit of the integration in Eq. (3) is chosen to be $I_p + 2U_p$ to ensure that all the integrated harmonics are well located in the plateaus for the moving H_2^+. Note that we have also calculated the wavelength scalings with the upper limit of $I_p + 3.17U_p$, which agree well with those with $I_p + 2U_p$ for both the moving and the static cases (except for a slight difference in the HHG yield). In Fig. 1, we show the wavelength-dependent HHG yield of H_2^+ simulated in the non-BO treatment (circles, moving H_2^+). For comparison, the result in the fixed-nucleus approximation (squares, static H_2^+) is also presented. Here the intensity of the driving laser pulse is 2.5×10^{14} W/cm^2. One can see that HHG from the static H_2^+ shows a rapid decrease in the yield as the laser wavelength increases. The wavelength scaling law is $\sim\lambda^{-5.7}$, which is very close to previous results [41,42] as well as the case in atoms [22–25]. By contrast, each harmonic from the moving H_2^+ shows a much higher yield [see, e.g., Fig. 2(b)] and the decrease in the wavelength-dependent HHG yield is significantly reduced. These results can be attributed to ionization enhancement induced by the nuclear motion in the moving case. As shown in Fig. 2(a), in the case of static H_2^+, the nuclear wave packet is restricted to the Franck-Condon (FC) region, where the ionization rate is inappreciable due to the higher ionization threshold (see Process 1). While in the moving case, the nuclear wave packet forced by the laser field can go beyond the FC region and move toward a larger internuclear distance (see Process 2), where the ionization rate is higher than that at equilibrium internuclear distance due to the lower ionization potential (see Process 3). The higher ionization rate therefore leads to an enhancement of the HHG yield in the moving case.

In order to check the above statement, we have plotted the harmonic spectra driven by the 1000-nm laser pulse for moving and static H_2^+ in Fig. 2(b). The overall intensity of the harmonics from the moving H_2^+ is about 1–2 orders of magnitude higher than that from the static H_2^+. Figures 2(c) and 2(d) show the time-frequency images of HHG from static and moving

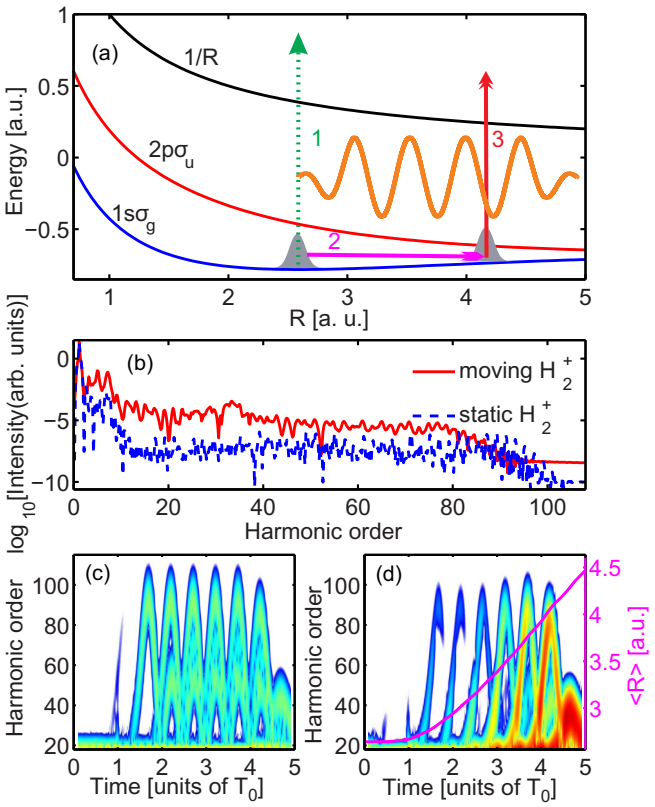

FIG. 2. (a) Mechanism of HHG enhancement in moving H_2^+. For static H_2^+, the ionization mainly occurs at the equilibrium distance, where the ionization threshold is high (Process 1). For moving H_2^+, the nuclear wave packet is forced to a larger internuclear distance (Process 2) and then the ionization occurs with a lower ionization threshold (Process 3). (b) Harmonic spectra driven by a 1000-nm laser pulse with an intensity of 2.5×10^{14} W/cm^2 for moving H_2^+ (solid line) and static H_2^+ (dashed line). (c) Time frequency analysis of the harmonic spectrum for static H_2^+ in (b). (d) Time frequency analysis of the harmonic spectrum for moving H_2^+ in (b), and time-dependent internuclear distance $\langle R(t)\rangle$ is also illustrated as the solid line.

H_2^+, respectively. It is obvious that the internuclear distance is maintained at R_e in the static case and the corresponding harmonic radiation within each half optical cycle from $1.5T_0$ to $5T_0$ (T_0 is the optical cycle of the driving laser pulse) has a comparable intensity. However, in the moving case, the internuclear distance $\langle R\rangle$ forced by the laser field increases gradually with time [solid line in Fig. 2(d)]. In the first $2.5T_0$, the harmonic radiation is inefficient due to the small internuclear distance, which is still close to the FC region. Afterwards, the internuclear distance is stretched far beyond the FC region, leading to more pronounced harmonic radiation at the last $2.5T_0$. The nuclear-motion-induced CREI effect is responsible for the enhancement of HHG in the moving case. Moreover, in our simulation the laser pulse has the same number of optical cycle for each wavelength. Driven by a longer wavelength laser, the nuclear wave packet can be stretched to a larger internuclear distance due to the longer time for dissociation, which will give rise to a larger ionization at longer wavelengths. This is demonstrated by the increasing wavelength-dependent ionization probability in Fig. 3(a). As a consequence, the

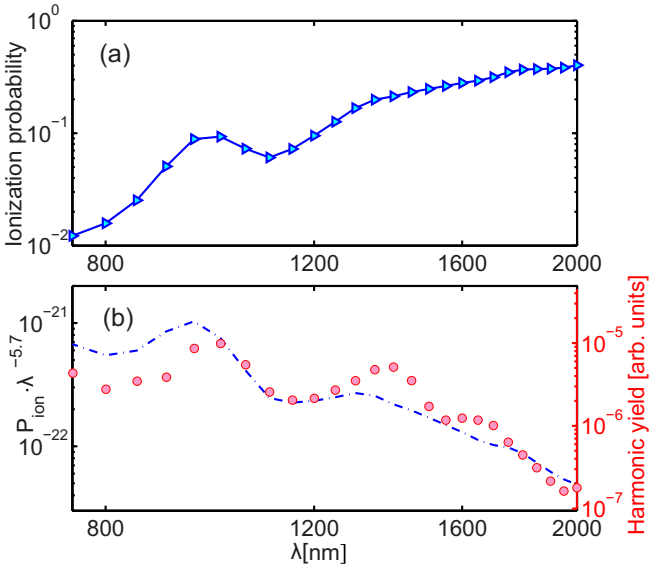

FIG. 3. (a) Ionization probability as a function of the laser wavelength. (b) Product of the wavelength-dependent ionization probability and the wavelength scaling $\sim\lambda^{-5.7}$ in static H_2^+. For comparison, the wavelength-dependence HHG yield in moving H_2^+ is also presented (circles).

decrease in the wavelength-dependent HHG yield in moving H_2^+ is reduced compared to that in the static case.

Apart from the slower downtrend, the wavelength scaling of HHG from moving H_2^+ also shows an oscillation structure in the range from 800 to 1600 nm. As shown in Fig. 1, two obvious peaks appear at 1000 and 1400 nm. This two-peak structure can be attributed to the oscillation in the R-dependent ionization probability of H_2^+ near the critical distance of the CREI [44,47,48]. In order to check this point, we have presented the ionization probability in moving H_2^+ as a function of the wavelength of the driving laser pulse in Fig. 3(a). One can see that the wavelength-dependent ionization probability exhibits a peak at 1000 nm and a shoulder at 1400 nm, which are consistent with those of the wavelength scaling shown in

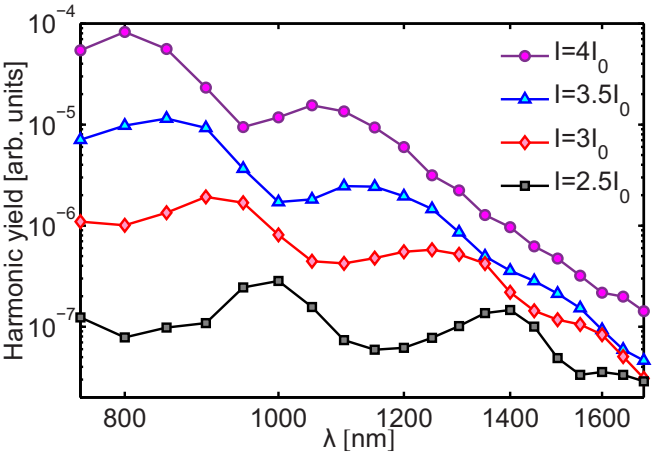

FIG. 4. Wavelength dependence of HHG yield for moving H_2^+ with the driving laser intensity of $2.5 \times I_0$, $3 \times I_0$, $3.5 \times I_0$, and $4 \times I_0$, where $I_0 = 1 \times 10^{14}$ W/cm^2. HHG yields are shifted for clarity.

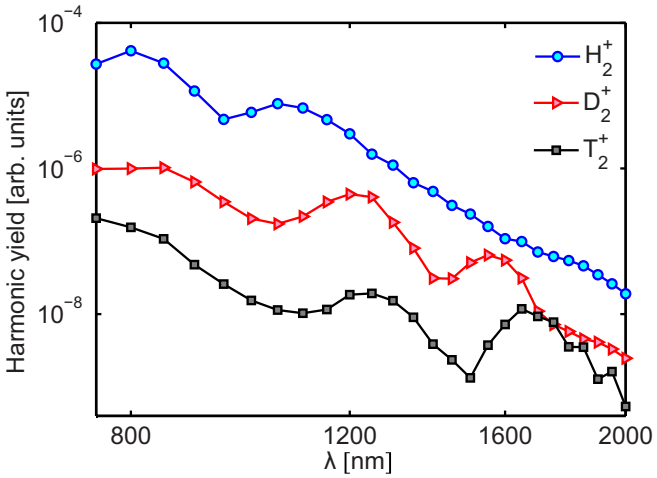

FIG. 5. Wavelength dependence of HHG yield for moving H_2^+, D_2^+, and T_2^+. Here the driving laser intensity is 4×10^{14} W/cm^2 and HHG yields are shifted for clarity.

Fig. 1. By multiplying the wavelength-dependent ionization probability to the wavelength scaling $\lambda^{-5.7}$ in static H_2^+, the obtained result [dashed line in Fig. 3(b)] has well reproduced the main structure of the wavelength scaling in the molecular H_2^+, except for the slight shift (50 nm) of the two peaks. This good agreement implies that the modulation in the wavelength scaling of moving H_2^+ indeed originates from the CREI effect induced by nuclear motion. Here, it is worth mentioning that the periodic oscillation in the wavelength scaling of HHG has also been discovered in atomic systems [23,24]. There the oscillation is attributed to effect of the quantum path interference, which is different from that in this paper.

For further check, we have also investigated the dependence of the wavelength scaling on the intensity of the driving laser pulse. As illustrated in Fig. 4, the two-peak structure shifts to a shorter wavelength as the peak intensity of the driving laser pulse increases from 2.5 to 4×10^{14} W/cm^2. This phenomenon can be understood by the picture of nuclear-motion-induced CREI. Since the nuclear motion driven by the laser pulse with a higher intensity is more rapid, it requires a much shorter time to reach the critical internuclear distance of CREI, which therefore corresponds to a shorter driving laser wavelength. Note that with an increasing laser intensity, the decrease in the wavelength-dependent HHG yield becomes more and more dramatic. This is due to the much faster depletion of the ground state at longer wavelengths for the higher laser intensity [43]. On the other hand, the isotope effect on the wavelength scaling is also studied. Figure 5 shows the wavelength scaling of the HHG yield for H_2^+, D_2^+, and T_2^+. One can see that the two-peak structure still exists in the wavelength scalings of D_2^+ and T_2^+. However, due to their heavier nuclear mass and therefore slower nuclear dissociation, it requires a much longer time to reach the critical distance for CREI. As a result, these two peaks move to much longer wavelengths of the driving laser pulse.

IV. CONCLUSION

In conclusion, we have investigated the wavelength scaling of HHG from H_2^+ by solving the non-BO TDSE. In comparison with the fixed-nucleus approximation, HHG from moving H_2^+ shows a much slower decrease in the wavelength scaling. This slower wavelength scaling is demonstrated to originate from the nuclear-motion-induced CREI effect, which has considerably enhanced the ionization rate and therefore the HHG yield at the longer laser wavelength due to the larger nuclear separation. Moreover, due to the oscillation in the R-dependent ionization rate, we also find an oscillation structure in the wavelength scaling of H_2^+. By increasing the laser intensity or the nuclear mass, the oscillation structure can be modulated towards shorter or longer wavelengths of the driving laser pulse. Our study will provide a valuable guideline for generating a harmonic spectrum with a high efficiency in the midinfrared regime.

ACKNOWLEDGMENTS

This work was supported by the National Natural Science Foundation of China under Grants No. 11627809, No. 11422435, No. 11234004, No. 11404123, No. 61275126, and No. 11704137, the Program for HUST Academic Frontier Youth Team, and a China Postdoctoral Science Foundation Funded Project (No. 2017M610467). Numerical simulations presented in this paper were carried out using the High Performance Computing experimental testbed in SCTS/CGCL (see http://grid.hust.edu.cn/hpcc).

[1] M.-C. Chen, P. Arpin, T. Popmintchev, M. Gerrity, B. Zhang, M. Seaberg, D. Popmintchev, M. M. Murnane, and H. C. Kapteyn, Phys. Rev. Lett. **105**, 173901 (2010).

[2] T. Popmintchev *et al.*, Science **336**, 1287 (2012); D. Popmintchev *et al.*, *ibid.* **350**, 1225 (2015).

[3] M. Hentschel, R. Kienberger, Ch. Spielmann, G. A. Reider, N. Milosevic, T. Brabec, P. Corkum, U. Heinzmann, M. Drescher, and F. Krausz, Nature (London) **414**, 509 (2001).

[4] E. Goulielmakis, M. Schultze, M. Hofstetter, V. S. Yakovlev, J. Gagnon, M. Uiberacker, A. L. Aquila, E. M. Gullikson, D. T. Attwood, R. Kienberger, F. Krausz, and U. Kleineberg, Science **320**, 1614 (2008).

[5] J. Li, X. Ren, Y. Yin, K. Zhao, A. Chew, Y. Cheng, E. Cunningham, Y. Wang, S. Hu, Y. Wu, M. Chini, and Z. Chang, Nat. Commun. **8**, 186 (2017).

[6] O. Kfir *et al.*, Nat. Photon. **9**, 99 (2014); T. Fan *et al.*, Proc. Natl. Acad. Sci. USA **112**, 14206 (2015).

[7] X. Zhang *et al.*, Opt. Lett. **42**, 1027 (2017); L. Li *et al.*, Opt. Quant. Electron **49**, 73 (2017); H. Yuan *et al.*, *ibid.* **49**, 214 (2017); J. Opt. Soc. Am. B **34**, 2390 (2017).

[8] J. Itatani, J. Levesque, D. Zeidler, H. Niikura, H. Pépin, J. C. Kieffer, P. B. Corkum, and D. M. Villeneuve, Nature **432**, 867 (2004).

[9] C. Zhai, X. Zhu, P. Lan, F. Wang, L. He, W. Shi, Y. Li, M. Li, Q. Zhang, and P. Lu, Phys. Rev. A **95**, 033420 (2017); Y. Li,

X. Zhu, P. Lan, Q. Zhang, M. Qin, and P. Lu, *ibid.* **89**, 045401 (2014).

[10] S. Haessler, J. Caillat, W. Boutu, C. Giovanetti-Teixeira, T. Ruchon, T. Auguste, Z. Diveki, P. Breger, A. Maquet, B. Carré, R. Taïeb, and P. Salières, Nat. Phys. **6**, 200 (2010).

[11] M. He *et al.*, Opt. Quant. Electron **49**, 232 (2017); X. Zhu *et al.*, Opt. Express **19**, 24198 (2011); Y. Li *et al.*, *ibid.* **25**, 11233 (2017); X. Liu, P. Li, X. Zhu, P. Lan, Q. Zhang, and P. Lu, Phys. Rev. A **95**, 033421 (2017).

[12] R. Kienberger *et al.*, Science **297**, 1144 (2002); Y. Pertot *et al.*, *ibid.* **355**, 264 (2017).

[13] M. Hohenleutner *et al.*, Nature **523**, 572 (2015); H. Liu *et al.*, Nat. Phys. **13**, 262 (2017).

[14] X. Liu, X. Zhu, P. Lan, X. Zhang, D. Wang, Q. Zhang, and P. Lu, Phys. Rev. A **95**, 063419 (2017); S. Wang *et al.*, Opt. Quant. Electron **49**, 389 (2017); S. Ke *et al.*, *ibid.* **49**, 224 (2017).

[15] M. Lewenstein, P. Balcou, M. Y. Ivanov, A. LHuillier, and P. B. Corkum, Phys. Rev. A **49**, 2117 (1994).

[16] P. B. Corkum, Phys. Rev. Lett. **71**, 1994 (1993).

[17] C. Vozzi, F. Calegari, E. Benedetti, S. Gasilov, G. Sansone, G. Cerullo, M. Nisoli, S. De Silvestri, and S. Stagira, Opt. Lett. **32**, 2957 (2007).

[18] D. Brida, G. Cirmi, C. Manzoni, S. Bonora, P. Villoresi, S. De Silvestri, and G. Cerullo, Opt. Lett. **13**, 741 (2008).

[19] Z. Hong *et al.*, Opt. Quant. Electron **49**, 392 (2017); Opt. Laser Technol. **98**, 169 (2018); S. A. Rezvani *et al.*, Opt. Lett. **42**, 3367 (2017).

[20] T. Popmintchev, M.-C. Chen, A. Bahabad, M. Gerrity, P. Sidorenko, O. Cohen, I. P. Christov, M. M. Murnane, and H. C. Kapteyn, Proc. Natl. Acad. Sci. USA **106**, 10516 (2009).

[21] E. J. Takahashi, T. Kanai, K. L. Ishikawa, Y. Nabekawa, and K. Midorikawa, Phys. Rev. Lett. **101**, 253901 (2008).

[22] J. Tate, T. Auguste, H. G. Muller, P. Salières, P. Agostini, and L. F. DiMauro, Phys. Rev. Lett. **98**, 013901 (2007).

[23] K. Schiessl, K. L. Ishikawa, E. Persson, and J. Burgdörfer, Phys. Rev. Lett. **99**, 253903 (2007).

[24] L. He, P. Lan, C. Zhai, Y. Li, Z. Wang, Q. Zhang, and P. Lu, Phys. Rev. A **91**, 023428 (2015); L. He, Z. Wang, Y. Li, Q. Zhang, P. Lan, and P. Lu, *ibid.* **88**, 053404 (2013).

[25] M. V. Frolov, N. L. Manakov, and A. F. Starace, Phys. Rev. Lett. **100**, 173001 (2008).

[26] P. Colosimo, G. Doumy, C. I. Blaga, J. Wheeler, C. Hauri, F. Catoire, J. Tate, R. Chirla, A. M. March, G. G. Paulus, H. G. Muller, P. Agostini, and L. F. DiMauro, Nat. Phys. **4**, 386 (2008).

[27] A. D. Shiner, C. Trallero-Herrero, N. Kajumba, H. C. Bandulet, D. Comtois, F. Légaré, M. Giguère, J. C. Kieffer, P. B. Corkum, and D. M. Villeneuve, Phys. Rev. Lett. **103**, 073902 (2009).

[28] J. Chen, B. Zeng, X. Liu, Y. Cheng, and Z. Xu, New J. Phys. **11**, 113021 (2009).

[29] P. Lan, E. J. Takahashi, and K. Midorikawa, Phys. Rev. A **81**, 061802 (2010).

[30] M. Lein, N. Hay, R. Velotta, J. P. Marangos, and P. L. Knight, Phys. Rev. Lett. **88**, 183903 (2002).

[31] S. Baker, J. S. Robinson, M. Lein, C. C. Chirilă, R. Torres, H. C. Bandulet, D. Comtois, J. C. Kieffer, D. M. Villeneuve, J. W. G. Tisch, and J. P. Marangos, Phys. Rev. Lett. **101**, 053901 (2008).

[32] T. Kanai, S. Minemoto, and H. Sakai, Nature (London) **435**, 470 (2005).

[33] C. Vozzi, F. Calegari, E. Benedetti, J.-P. Caumes, G. Sansone, S. Stagira, M. Nisoli, R. Torres, E. Heesel, N. Kajumba, J. P. Marangos, C. Altucci, and R. Velotta, Phys. Rev. Lett. **95**, 153902 (2005).

[34] O. Smirnova, Y. Mairesse, S. Patchkovskii, N. Dudovich, D. Villeneuve, P. Corkum, and M. Y. Ivanov, Nature **460**, 972 (2009).

[35] P. M. Kraus, D. Baykusheva, and H. J. Wörner, Phys. Rev. Lett. **113**, 023001 (2014).

[36] M. Lein, Phys. Rev. Lett. **94**, 053004 (2005).

[37] S. Baker, J. S. Robinson, C. A. Haworth, H. Teng, R. A. Smith, C. C. Chirilă, M. Lein, J. W. G. Tisch, and J. P. Marangos, Science **312**, 424 (2006).

[38] P. Lan, M. Ruhmann, L. He, C. Zhai, F. Wang, X. Zhu, Q. Zhang, Y. Zhou, M. Li, M. Lein, and P. Lu, Phys. Rev. Lett. **119**, 033201 (2017).

[39] X.-B. Bian and A. D. Bandrauk, Phys. Rev. Lett. **113**, 193901 (2014).

[40] X. Yuan, P. Wei, C. Liu, X. Ge, Y. Zheng, Z. Zeng, and R. Li, Opt. Express **24**, 8194 (2016).

[41] Y. Li, S. Yu, X. Duan, Y. Shi, and Y. Chen, J. Phys. B **49**, 075603 (2016).

[42] S. Yue, H. Du, H. Wu, J. Li, and B. Hu, Chem. Phys. **494**, 56 (2017).

[43] C. Liu, Z. Zeng, P. Wei, P. Liu, R. Li, and Z. Xu, Phys. Rev. A **81**, 033426 (2010).

[44] T. Zuo and A. D. Bandrauk, Phys. Rev. A **52**, R2511(R) (1995).

[45] T. Seideman, M. Yu. Ivanov, and P. B. Corkum, Phys. Rev. Lett. **75**, 2819 (1995).

[46] T. Pfeifer, D. Walter, G. Gerber, M. Yu. Emelin, M. Yu. Ryabikin, M. D. Chernobrovtseva, and A. M. Sergeev, Phys. Rev. A **70**, 013805 (2004).

[47] M. Y. Emelin, M. Y. Ryabikin, and A. M. Sergeev, New J. Phys. **10**, 025026 (2008).

[48] X.-B. Bian, L.-Y. Peng, and T.-Y. Shi, Phys. Rev. A **77**, 063415 (2008).

[49] M. Lara-Astiaso, R. E. F. Silva, A. Gubaydullin, P. Rivière, C. Meier, and F. Martín, Phys. Rev. Lett. **117**, 093003 (2016).

[50] B. Wang, L. He, F. Wang, H. Yuan, X. Zhu, P. Lan, and P. Lu, Opt. Express **25**, 17777 (2017).

[51] K. C. Kulander, F. H. Mies, and K. J. Schafer, Phys. Rev. A **53**, 2562 (1996).

[52] K. Liu, W. Hong, Q. Zhang, and P. Lu, Opt. Express **19**, 26359 (2011).